Detection of fiber orientation from experimental strain field using data driven neural network

Chengyang Mo

ENM 531 Spring 2019

1 Introduction

The rise of various methods in 3d printing has been essential to material and structure development. Particularly, the introduction of direct ink writing method [1, 2, 3] provides capability to print far more various material compared to fused deposition modelling which limits the material to be thermoplastic. Specifically, it is used to print structures with various fiber composites including Epoxy/carbon fiber system [2, 3] and Poly-dimethylsiloxane(PDMS)/glass fiber system [4]. Addtion of fibers in matrix can drastically increase mechanical properties with increasing fiber content.

Moreover, manufacturing fiber composite with 3d printing methods allow us locally control the microstructure which can not be achieved in conventional composite manufacturing using casting and prepeg layup. This local control can be achieved via printing path optimization [2, 5] or intricate nozzle design turning on/off locally mixing or rotation[3]. With the ability to tune local properties, it is the right time to ask what is the best way to print some fiber composite structure to obtain the best properties. Microstructural design with the purpose of optimizing properties has been studied recently with machine learning techniques for polycrystalline metals and microstructure reconstruction with Transfer learning [6].

However, it is important to first understand the local microstructure created in these printing methods. To characterize local microstructure, usually some optical or particle method is used. However, optical method is usually great for macroscale objects while particle method is great for nanoscale objects. The fiber composites we are interested lies in a tricky part between macroscale and nanoscale where either method is great for characterizing its microstructure. And in this report, I will propose a method to obtain full field local microstructure information from experimentally obtained strain field during loading. I will do that by invoking equation of elasticity and introduction of neural network of latent variable.

I will train a transposed convolutional neural network to generate 2D orientation mapping within a printed structure. The network will be trained with experimentally obtained strain map of the sample during small elastic tensile loading. The strain information is used to ensure the generated orientation map will satisfy the equation of elasticity.

2 Background and Theory

2.1 3D Printing

The material system we are interested here is material printed with PDMS and glass fiber [4]. The material is mixed in a vacuum mixer and then transferred to a syringe. The syringe is then mounted on a modified commercial 3d printer with a nozzle of 400 μm. Material is printed under pressure in design pattern. A motor is attached to the nozzle to allow rotation. Due to the shear stress between the ink and the wall of the nozzle during printing, the fibers within the ink is aligned with direction of the movement of the nozzle. However if rotation is turned on, it was found the fiber forms helical structures within each filament printed with the fibers close to the outer wall not aligned with the printing direction [3]

2.2 Equation of Elasticity

A solid deformable body has to satisfy the equations of elasticity which consist of four major components. The first of which is the equation of kinematics which describe the relation between displacement and strain:

$$\epsilon_{ij} = \frac{1}{2}(u_{i,j} + u_{j,i}) \tag{1}$$

Where u is the displacement of the body in 3 dimensional space and ϵ is a 2nd order tensor which describe strain exerted on the body. The second set of equation map local forces to local stress components as following:

$$t_i = \sigma_{ij} n_j \tag{2}$$

where σ is a 2nd order tensor describing the stress state of the body, t is the local forces exerted on a point and n is the normal vector of the point within the body. Next, all deformable body must satisfy static equilibrium:

$$\sigma_{ij,j} + b_i = 0 \tag{3}$$

Where b_i is the body force. Lastly, the relation between the stress and strain is called the constitutive equations:

$$\sigma_{ij} = C_{ijkl} \epsilon_{kl} \tag{4}$$

C is a fourth order tensor usually. However, some results of equilibrium also guarantees stress to be symmetric and by definition strain ϵ is a symmetric tensor. Hence in 3d, there are only 6 unique components in both *sigma* and *epsilon*. This result simplifies the stiffness tensor C from fourth order with 3 dimension to a second order tensor S of seconder order and 6 dimensions:

$$\sigma_i = S_{ij}\epsilon_j \tag{5}$$

Additionally, using energy method, the equation of elasticity with a boundary value can be satisfied when the potential energy within a region:

$$\Pi = \int_B \sigma_{ij}\epsilon_{ij} dV + \int_{\partial B} t_i u_i dA \tag{6}$$

is minimized. And this relation would be crucial in our approach as this is a scalar that can be related to the loss function of our network.

2.3 Fiber Composite Theory

With a structure for our loss function defined, we are still missing a step defining the constitutive relation of our material. This is a well studied area with theoretical results that can help us defining the determinant process. I will use the model proposed by Halpin and Tsai [7]. In this model, for a given volume fraction of fiber composites with isotropic materials properties (E_f, E_m, μ_f, μ_m). Under plane strain loading condition, the stiffness matrix can be expressed as:

$$S = \begin{bmatrix} S_{11} & S_{12} & 0 \\ S_{12} & S_{22} & 0 \\ 0 & 0 & S_{66} \end{bmatrix} \tag{7}$$

where all the components of S can be computed with the material properties and volume fraction of fiber ϕ.

Locally, stiffness matrix may require transformation according to the fiber orientation as in the previous setup, fiber is usually oriented in the local 1 direction. To obtain local stiffness matrix, transformation of the stiffness matrix is required. Since the matrix here is modified from proper tensors, the proper transformation rule does not apply here. Rather in 2D space to transform the local stiffness matrix with a transformation angle of θ is defiend by:

$$S' = R(\theta)BR^{-1}(\theta)SB^{-1} \tag{8}$$

where R is the standard rotational matrix in 2D with rotation angle θ and B is a diagonal matrix with its diagonal components being 1,1,2 respectively.

2.4 Digital Image Correlation

Experimentally, we obtain full field strain map of the sample via digital image correlation (DIC). DIC is an experimental technique which tracks the motion of subset of pixels through cross correlation. The algorithm is accurate up to sub pixel scale in the measured displacement. With the obtained displacement field, full field strain data can then be computed as described by equation 1.

3 Network Architecture

The network architecture is described in Figure 1. The orientation P will be generated from a random latent variable Z with some distribution function $P(Z)$. A transposed CNN or Upsampling (f_θ) is built to tranform the latent variable to the P space. Then a determinant process using the theory of fiber composite described in previous section will provide as the local stiffness matrix as a 3x3 matrix. Then the training will be done by minimizing the

Potential energy described in Equation. 6 with experimentally obtained strain as input.

The latent Z space is sampled from a standard normal distribution with 0 mean. The P space spans from 0° to 90°. Scaling is done by a sigmoid activation function in the last layer of the generator and sequentially multiplied by 90.

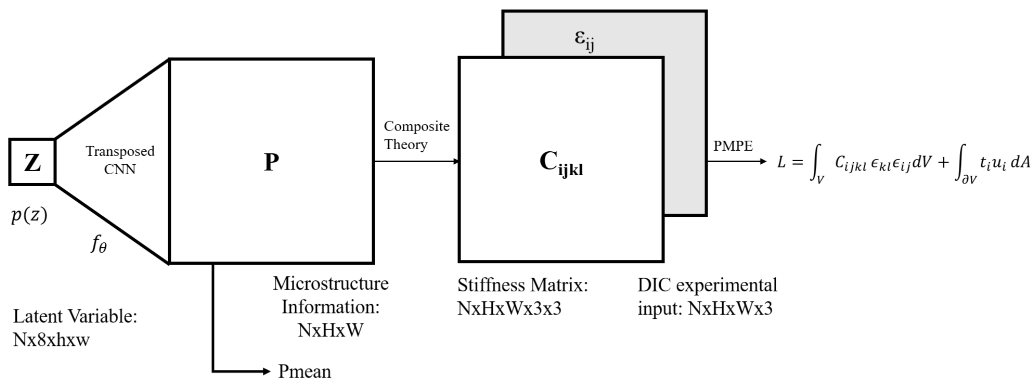

Figure 1: Framework of the model

The latent Z space has a dimension of N×8×10×1. The network consists of three transposed CNN layers with kernel sizes of 6,5 and 6 respectively. Paddings are adjusted so that the final P space have the same dimensions as the strain input of N×92×10. A decoder f_ϕ is also constructed to map back to Z from P. A normal CNN structures is used.

4 Result

I have conducted 15 experiments with samples 3d printed with two different fiber content (3% and 5%). Three of those experiments are printed with rotational nozzle. The experimentally obtained strain map is shown in Figure 2. The overall tensile strain throughout the sample is $\sim 5\%$.

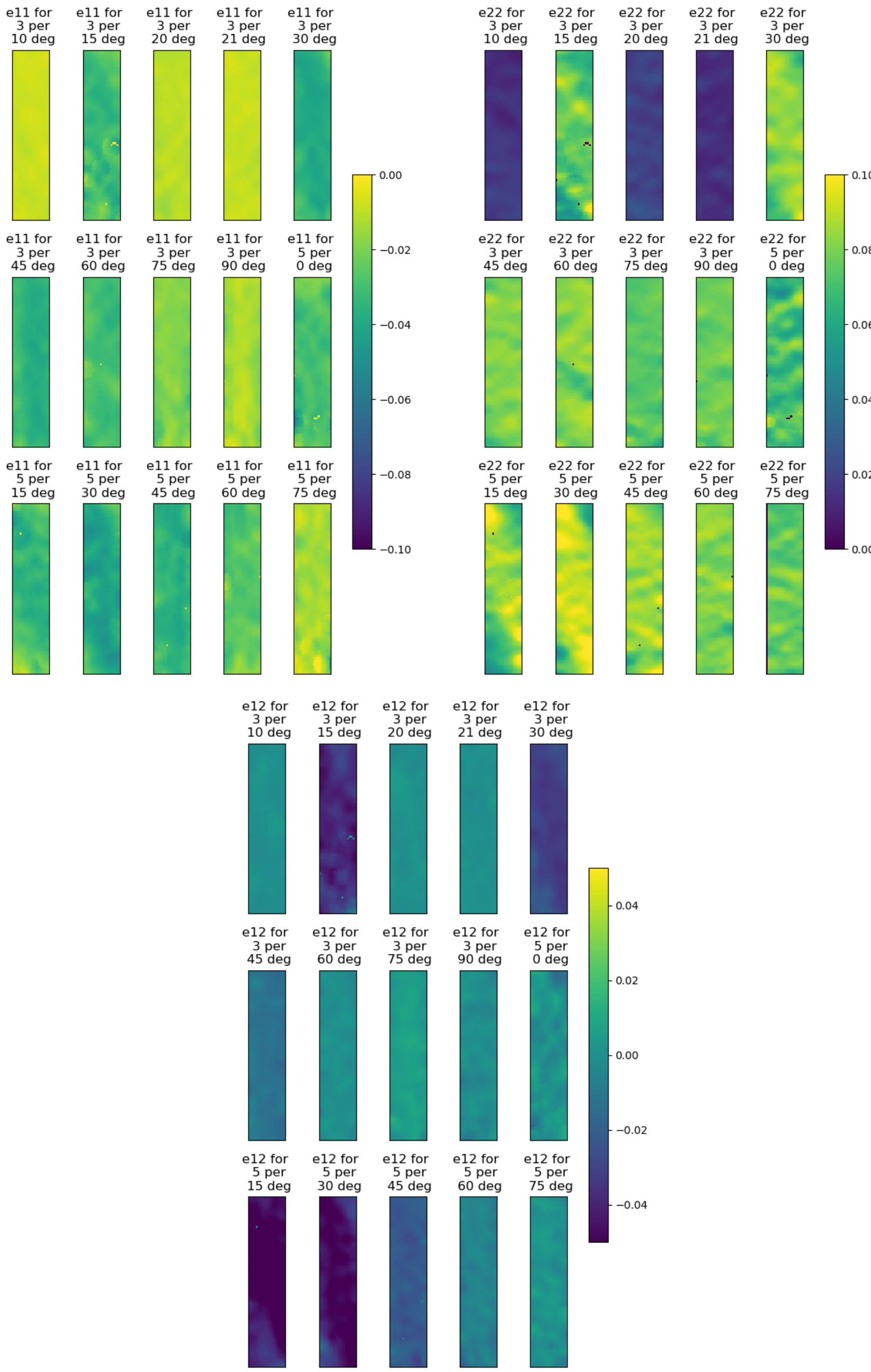

Figure 2: Strain map of all samples tested

With the obtained strain data set, the result of first training is not ideal. The training shows fast decreasing loss function while the orientation map shows little perturbation and concentrate around 45 degrees. 45 degree corresponds to the 0 in the latent space. This resembles modal collapses observed in training of Generative Adversarial Networks (GAN). Then few methods to mitigate such modal collapses is experimented.

Firstly, additional data are generated by data augmentation. Additional displacement and strain data is created by adding random noise on the original displacement data. The strain data is then calculated from the noised displacement data via Equation 1. By doing so, additional training data is added. Secondly, a decoder is added to the network attempting to regularized the modal collapse. The decoder maps the generated P space back to the Z space. An additional term is added to the loss function.

$$L_{decoder} = ||Z^* - Z|| \tag{9}$$

Thirdly, parameters are regularized in the CNN where batch normalization is added as well as dropouts.

After a few iterations of fine tuning hyper parameters, the result does not improve much. Though the variance within each sample increase largely compared to the initial implementation. The final result is shown in Figure 3. Figure 3a shows the initial result without any regularization. Figure 3b shows the result with 10% dropout rate and additional decoder loss function. The generated sample is no longer homogeneous with very large variation in the orientation within the sample due to the dropout process. However, the result does not accurately predict the orientation and the loss function does not converge to a low value. Figure 3c shows result of additional augmented sample from the original data set. The addition of augmentation also promote irregularity within the generated sample but still failed at accurate prediction. Lastly, Figure 3 shows the result with 5000 training iterations with dropout rate of 10% and 100 additional augmented data per original data set (a total sample size of 15000) trained in batches (batch size of 100). Surprisingly with increase augmentation, the result does not improve, seemingly worse than less augmentation as the orientation seems rather homogeneous.

In conclusion, I propose an approach to obtain fiber orientation map in a 3d printed PDMS glass fiber composite system using data driven experimental input of full field strain map. The approach of generative network causes issues in the training process, leading to mode collapses of the desired output. A few techniques such as data augmentation, dropout of network and decoder loss are implemented to try separate the modes. However, the attempts are not successful in creating desired results. In future work, a simpler system could be implemented in order to test the feasibility of the proposed architecture. The fiber orientation of such system should be easily obtainable so that it can be used as part of the training. A potential candidate could be conventional layup fiber composites. Moreover, additional experiments can be conducted to generate additional samples may help the training process.

References

[1] Jordan R. Raney and Jennifer A. Lewis. Printing mesoscale architectures. *MRS Bulletin*, 40(11):943–950, 2015.

[2] Sardar Malek, Jordan R. Raney, Jennifer A. Lewis, and Lorna J. Gibson. Lightweight 3D cellular composites inspired by balsa. *Bioinspiration and Biomimetics*, 12(2):aa6028, 2017.

[3] Jordan R Raney, Brett G Compton, Jochen Mueller, Thomas J Ober, Kristina Shea, and Jennifer A Lewis. Rotational 3D printing of damage-tolerant composites with programmable mechanics. *Proceedings of the National Academy of Sciences of the United States of America*, 115(6):1198–1203, 2018.

[4] Yijie Jiang, Lucia M Korpas, and Jordan R Raney. Bifurcation-based embodied logic and autonomous actuation. *Nature Communications*, 10(1), 2019.

[5] Grace X. Gu, Susan Wettermark, and Markus J. Buehler. Algorithm-driven design of fracture resistant composite materials realized through additive manufacturing. *Additive Manufacturing*, 17:47–54, 2017.

[6] Xiaolin Li, Yichi Zhang, He Zhao, Craig Burkhart, L Catherine Brinson, and Wei Chen. A Transfer Learning Approach for Microstructure Reconstruction and Structure-property Predictions. *Scientific Reports*, 8(1):1–13, 2018.

[7] J. C. Halpin and J. L. Kardos. The Halpin-Tsai Equations: A Review. *Polymer Engineering and Science*, 16(5), 1976.

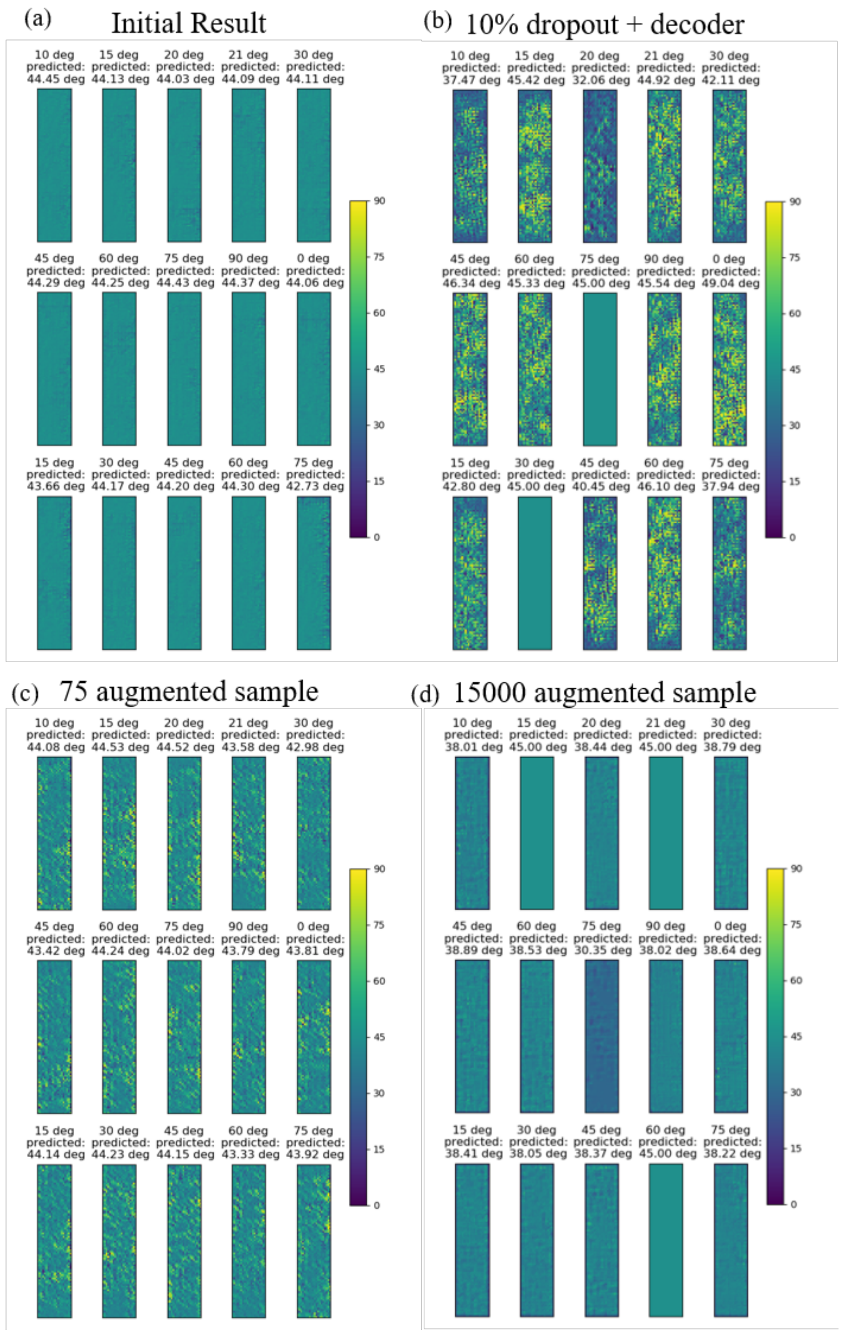

Figure 3: Final result of various attempt in regularizing the training